Clinical Immunology 198 (2019) 79–88

Contents lists available at ScienceDirect

Clinical Immunology

journal homepage: www.elsevier.com/locate/yclim

Treg/Th17 imbalance is associated with poor autoimmune hepatitis prognosis

Yuli Liu[a,b], Weiming Yan[a,*], Wei Yuan[a], Peng Wang[a], Da Huang[a], Xiaoping Luo[c], Qin Ning[a,d,*]

[a] Institute of Infectious Disease, Tongji Hospital of Tongji Medical College, Huazhong University of Science and Technology, Wuhan, Hubei 430030, China
[b] Department of Gynecology, Hubei Women and Children's Hospital, Wuhan, Hubei 430070, China
[c] Department of Paediatrics, Tongji Hospital of Tongji Medical College, Huazhong University of Science and Technology, 430030 Wuhan, Hubei, China
[d] Department of Infectious Disease, Tongji Hospital of Tongji Medical College, Huazhong University of Science and Technology, 430030 Wuhan, Hubei, China

1. Introduction

Autoimmune hepatitis (AIH) is a liver-targeting autoimmune disease that is diagnosed most commonly in females, based on the presence of autoantibodies, increased levels of immunoglobulin G (IgG), and interface hepatitis, as well as the absence of viral hepatitis, according to criteria established by the International AIH Group (IAIHG) [1]. Two types of AIH are distinguished according to antibodies present: type1 (AIH-1), based on serum positivity for anti-smooth muscle and/or anti-nuclear antibodies (ANA), and type 2 (AIH-2), based on serum positivity for anti-liver-kidney microsomal type 1 (LKM-1) and/or anti-liver cytosol type 1 (LC1) antibodies [2]. The anti-LKM-1 autoantigen has been identified as cytochrome P4502D6 (CYP2D6), which is expressed mainly by hepatocytes. Previous studies have suggested that anti-LKM-1 may contribute to autoimmune destruction of the liver [3]. Like many other autoimmune diseases, AIH generally responds to immunosuppressive treatment, which should be instituted as soon as the diagnosis is made. If left untreated, AIH usually progresses to liver failure and requires transplantation [4].The etiology of AIH remains unclear, although both genetic and environmental factors are involved. Immune reactions against liver host antigens accompanied by dysregulation of immunoregulatory are believed to be the major mechanisms of liver damage.

$CD4^+$ $CD25^+$ $Foxp3^+$ regulatory T cells (Tregs) play a crucial role in the maintenance of immune balance to prevent autoimmune disease. Documented mechanisms of autoimmune suppression include cell-to-cell contact with antigen-presenting cells, metabolic disruption of effector T cell function, and secretion of anti-inflammatory cytokines [5]. The suppressive function of Tregs has been shown to be mediated by transforming growth factor-β (TGF-β) or fibrinogen-like protein 2 (Fgl2) in many models of inflammation [6,7]. By contrast, IL-17-producing Th cells (Th17) are a new member of the T-helper effector cell family that can induce inflammation and autoimmune tissue injury by producing proinflammatory cytokines, including interleukin-17 (IL-17A), IL-17F, IL-22, and IL-21 [8]. Among these cytokines, IL-17A and IL-22 are regarded the main effector cytokines [8] and have been implicated in the pathogenesis of several autoimmune diseases [9], including type 1 diabetes (T1D) and systemic lupus erythematosus (SLE) [10,11].

Recently, some studies have indicated that both peripheral Tregs and Th17 cells might play important roles in the pathogenesis of AIH [12–14]. However, the lack of an appropriate animal model has restricted insights into immunogical features of specialized Tregs or Th17 cells that reside in the liver. Thus, the association between hepatic Tregs or Th17 cells and AIH progression is still under discussion. In the present study, we investigated the dynamic balance of Treg/Th17 in the liver using an AIH murine model induced by human CYP2D6 [15], as well as the peripheral Treg/Th17 balance in 16 AIH patients. Our results highlight the importance of a decreased Treg/Th17 ratio in the immunopathogenesis of AIH and suggest Tregs as a potential target for AIH immunotherapy.

2. Material and method

2.1. Animals

Four-week-old female C57BL/6 (B6) mice used in this study were purchased from Huafukang Bioscience Company (Beijing, China) and maintained in specific pathogen-free conditions of an animal facility at the Institute of Infectious Disease of Tongji Hospital. Animal handling

Abbreviations: Tregs, $CD4^+$ $CD25^+$ $Foxp3^+$ regulatory T cells; Th17, IL-17-producing Th cells; AIH, autoimmune hepatitis; CYP2D6, cytochrome P4502D6; AD-2D6, adenovirus vector containing CYP2D6; anti-LKM-1, anti–liver-kidney microsomal type 1; LMNCs, liver mononuclear cells

* Corresponding author at: Address: No. 1095, Jiefang Avenue, 430030 Wuhan, China
E-mail addresses: ywm_net@qq.com (W. Yan), qning@vip.sina.com (Q. Ning).

https://doi.org/10.1016/j.clim.2018.11.003
Received 17 May 2018; Received in revised form 4 October 2018; Accepted 9 November 2018
Available online 16 November 2018
1521-6616/

protocols and experimental procedures conformed to the guidelines outlined in the Guide for the Care and Use of Laboratory Animals.

2.2. Patients

Sixteen female patients from the Department of Infectious Diseases, Tongji Hospital, who were diagnosed with probable or definite AIH between 2015 and 2016 according to the simplified IAIHG scoring system, were included in this study. Written informed consents were obtained from all participates. Available clinical and laboratory information were retrospectively analyzed, with samples from eight anonymous healthy female volunteers analyzed as the control group. Liver biopsies from two AIH patients were collected for histological evaluation, and normal liver tissue surrounding a hepatic cavernous hemangioma, obtained from a patient who underwent liver transplantation, served as a normal control.

2.3. Establishment of the AIH-2 murine model

Adenovirus vector-expressing human cytochrome P450 2D6 (AD-2D6) or green fluorescence protein (AD-GFP) at a concentration of 2×10^{10} pfu/mL were packaged and concentrated by Biowit Technologies (Shenzhen, China). B6 mice were immunized with a total volume of 100 μL AD-2D6 or AD-GFP virus solution intravenously and intraperitoneally to establish an AIH-2 murine model ($N = 5$/group/point-in-time) and control model (N = 5/group/point-in-time), respectively.

2.4. Preparation of mouse liver homogenates

Mouse liver samples were homogenized in phosphate-buffered saline (PBS) at 4 °C with a glass homogenizer. The crude homogenates were centrifuged at 500 × g for 10 min, and the supernatants were then analyzed for various cytokines by enzyme-linked immunosorbent assay (ELISA).

2.5. ELISA

The levels of serum total IgG (BETHYL, USA, cat. E99-131) and inflammatory cytokines (IL-17A and IL-22) in liver homogenates were analyzed by commercially available ELISA kit (NeoBioscience, China, cat. EMC008, EMC119) according to the manufacturer's instructions. Serum samples diluted 1:20 were prepared for a quantification of anti-CYP2D6 antibodies. Briefly, serum samples were introduced into coated microwell plates (LKM-1 Ab ELISA Kit, Abnova, Taiwan, cat. KA1280). The presence of anti-CYP2D6 antibodies was revealed by incubation with anti-mouse IgG/ALP-conjugated antibodies at a dilution of 1:2000 (ELISA helper kit, Dakewe Biotech, China, cat. DKW-F1). Colour was developed by incubation with phosphatase substrate *p*-nitrophenyl phosphate. Optical densities (ODs) were read at 405 nm using an ELISA reader (iMark Microplate Reader, BIO-RAD, USA).

2.6. Hematoxylin-eosin (H&E) staining

Liver specimens were fixed in 10% buffered formalin and embedded in paraffin. Sections (4-μm) were prepared, stained with H&E, and examined under a light microscope.

2.7. Immunohistochemical (IHC) analysis

Human CYP2D6 (hCYP2D6) expression and histological localization was investigated in formalin-fixed, paraffin-embedded liver tissue samples from AD-2D6 mice at one-week post infection. Liver tissues were incubated with a polyclonal antibody against hCYP2D6 (Sigma, Germany, cat. HPA045223) at a dilution of 1:250 in PBS at 4 °C for 12 h following incubation with commercially biotin-labeled goat anti-rabbit IgG antibodies (ZSGB-BIO, Beijing, China, cat. SP-9000).

2.8. Indirect immunofluorescence analysis

For the qualitative detection of anti-CYP2D6 antibodies during the establishment of animal model, formalin-fixed, paraffin-embedded rat liver and kidney sections were incubated with mouse sera diluted at 1:5, followed by incubation with Alexa Fluor 488-conjugated anti-mouse IgG secondary antibody (Abcam, UK, cat. Ab150077) diluted 1:500 and examined by immunofluorescence microscopy.

2.9. Isolation of liver mononuclear cells (LMNCs)

Prior to harvesting tissue, mouse livers were perfused with sterile PBS through the portal vein and weighed. Liver cell suspensions were prepared by grinding the liver tissues with a glass pestle. After filtering cells through a 200-gauge stainless steel mesh, cells were re-suspended in 40% Percoll (GE Healthcare, Piscataway, NJ, cat.17–0891-01) and centrifuged at 1500 × *g* for 30 min. LMNCs were harvested from the sediments.

2.10. Multi-colour flow cytometric assay

In addition to Fgl2 monoclonal antibody (Abnova, Taiwan, cat. H00010875-M01) and phycoerythrin (PE)-conjugated anti-mouse IgG antibody (BioLegend, CA, cat. 405,307), PE-conjugated anti-mouse IL-17 (cat. 559,502), PE-conjugated anti-mouse Foxp3 (cat. 560,414), PE-conjugated anti-mouse TGF-β (cat. 563,143), and their isotype controls were purchased from BD Biosciences (USA). Fluorescein isothiocyanate (FITC)-conjugated anti-human CD4 (cat. 11-0049-41), allophycocyanin (APC)-conjugated anti-human CD25 (cat. 17-0259-42), PE-conjugated anti-human CD127 (cat. 12-1278-42), APC-conjugated anti-human CD4 (cat. 17-0049-42), PE-conjugated anti- human IL17 (cat. 12-7179-42), and their isotype controls were purchased from eBioscience (USA). Cells were stained with fluorochrome- conjugated antibodies against surface receptors according to the standard procedure of BD Pharmingen. Fixation and permeabilization was performed using Foxp3 Fix/Perm Buffer Set (BioLegend, USA, cat.421403) and cells were then stained with the respective intracellular antibodies for 45 min at room temperature. For detection of Th17 intracellular cytokines, whole blood samples or LMNCs suspended in RPMI 1640 medium supplemented with 10% fetal bovine serum were stimulated with a cell stimulation cocktail (eBioscience, USA, cat.00-4975) containing phorbol-12-myristate-13-acetate (PMA, 50 ng/mL), ionomycin (1 μg/mL), and monensin (2 μg/mL) at 37 °C with 5% CO_2 for 5 h, followed by treatment with RBC lysis buffer (BD, USA, cat. 555,899) and/or incubation with fluorescently labeled anti-CD4 and anti- IL-17 antibodies. All samples were detected using a BD FACS Canto II Flow Cytometry System (BD, USA) and analyzed with BD FACS Diva Software.

2.11. Isolation and adoptive transfer of $CD4^+$ $CD25^+$ Treg cells

$CD4^+CD25^+$ Tregs were sorted by magnetic beads separation kit (Miltenyi Biotech, Germany, cat. 130-091-041) from splenocytes of healthy mice according to the manufacturer's instructions. $CD4^+CD25^+$ T cell suspensions with a purity > 90% (3×10^6 cells in 1 mL normal saline) were adoptively transferred to mouse livers via high-pressure tail vein injection at week 2 and week 3 post infection with AD-2D6 virus solution. AD-2D6 mice in the control group were injected with the same volume of saline at week 2 and week 3 ($N = 5$/group). Serum samples and liver tissues were collected from all the mice at week 4 post infection.

2.12. Statistical analysis

Data analysis was performed using SPSS 17.0 software and

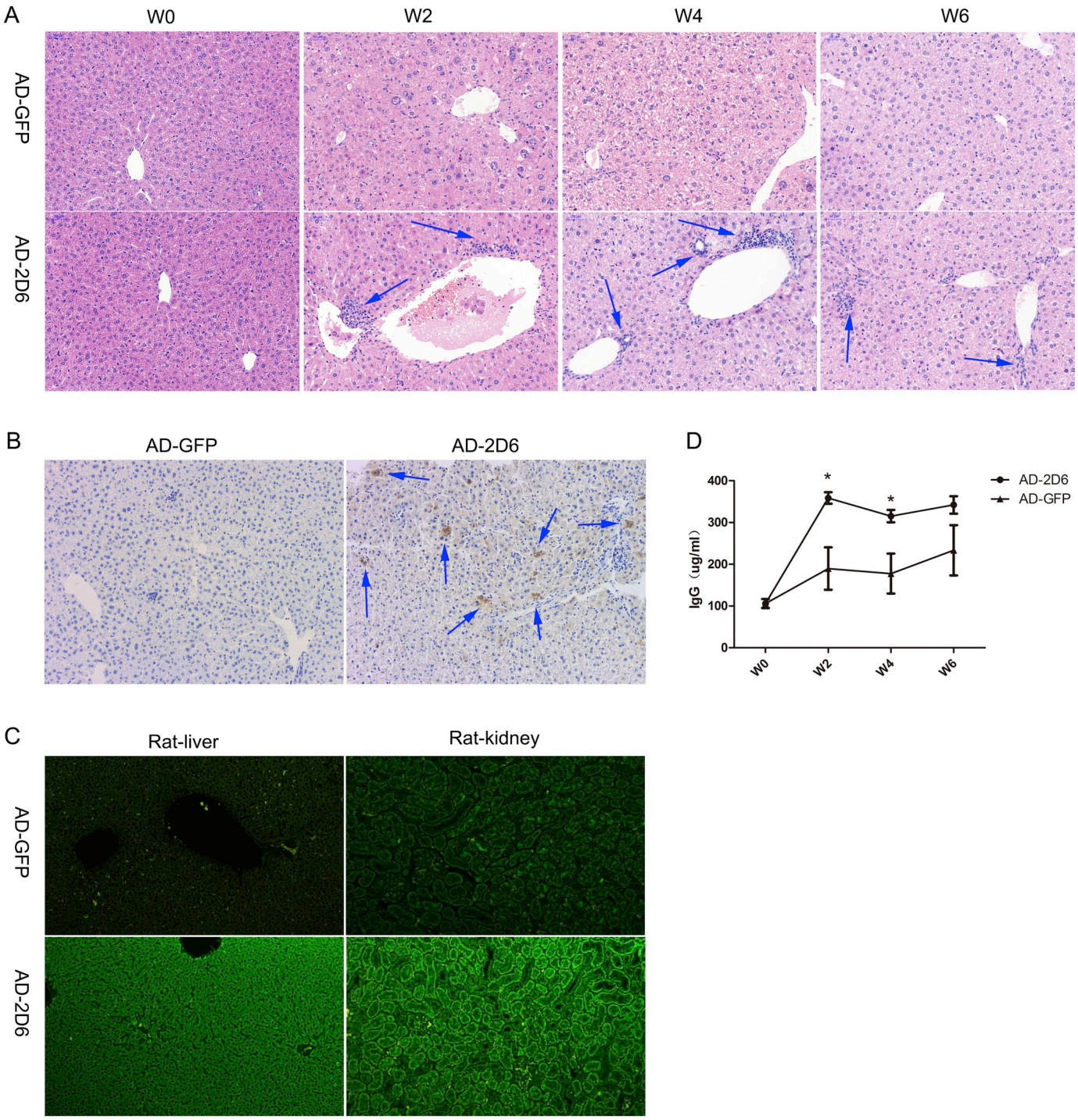

Fig. 1. Infection with AD-2D6 resulted in persistent autoimmune hepatitis. (A) Representative HE staining of the liver tissues of AD-2D6 and AD-GFP mice: a moderate interface hepatitis (blue arrows) was seen in AD-2D6 mice at week 2, 4, and 6 post infection (magnification, × 200). (B) The expression of CYP2D6 in the liver of AD-2D6 and AD-GFP mice at 1 weeks after immunization by IHC: only AD-2D6 mice showed the expression of CYP2D6 (blue arrows, magnification, × 200). (C) The expression of autoantibody against CYP2D6 (LKM-1) in the serum of AD-2D6 mice and AD-GFP mice at 4 weeks after immunization by indirect immunofluorescence analysis: only AD-2D6 mice showed the expression of LKM-1 (green fluorescence, magnification, × 400). (D) Comparison of titers of total IgG in the sera of AD-2D6 mice and AD-GFP mice at 0 (before immunization), 2, 4 and 6 weeks after immunization by ELISA. $N = 5$/group/point-in-time; $^*p < 0.05$ compared between the two groups at the same time point. (For interpretation of the references to colour in this figure legend, the reader is referred to the web version of this article.)

GraphPad Prism 5 version 5.01 software. The results were analyzed using an unpaired two-tailed Student's *t*-test or one-way analysis of variance as appropriate. All data were expressed as the mean ± standard error of the mean (SEM). A p value < 0.05 was considered statistically significant.

3. Results

3.1. Infection with AD-2D6 resulted in persistent autoimmune hepatitis

To assess this AIH murine model, both AD-2D6 mice and AD-GFP

mice were sacrificed at week 2, 4, and 6 post infection, and their liver injuries were evaluated. At week 2, AD-2D6 mice showed significantly moderate interface hepatitis, which was characterized by obvious inflammatory changes in hepatocytes around the portal area and central vein and progressive necrosis compared with mice infected with AD-GFP, with an expansion in these changes at weeks 4 and 6 (Fig. 1A). A definite expression of CYP2D6 was observed by IHC in the hepatocytes of AD-2D6 mice at week 1 post immunization, suggesting that the livers

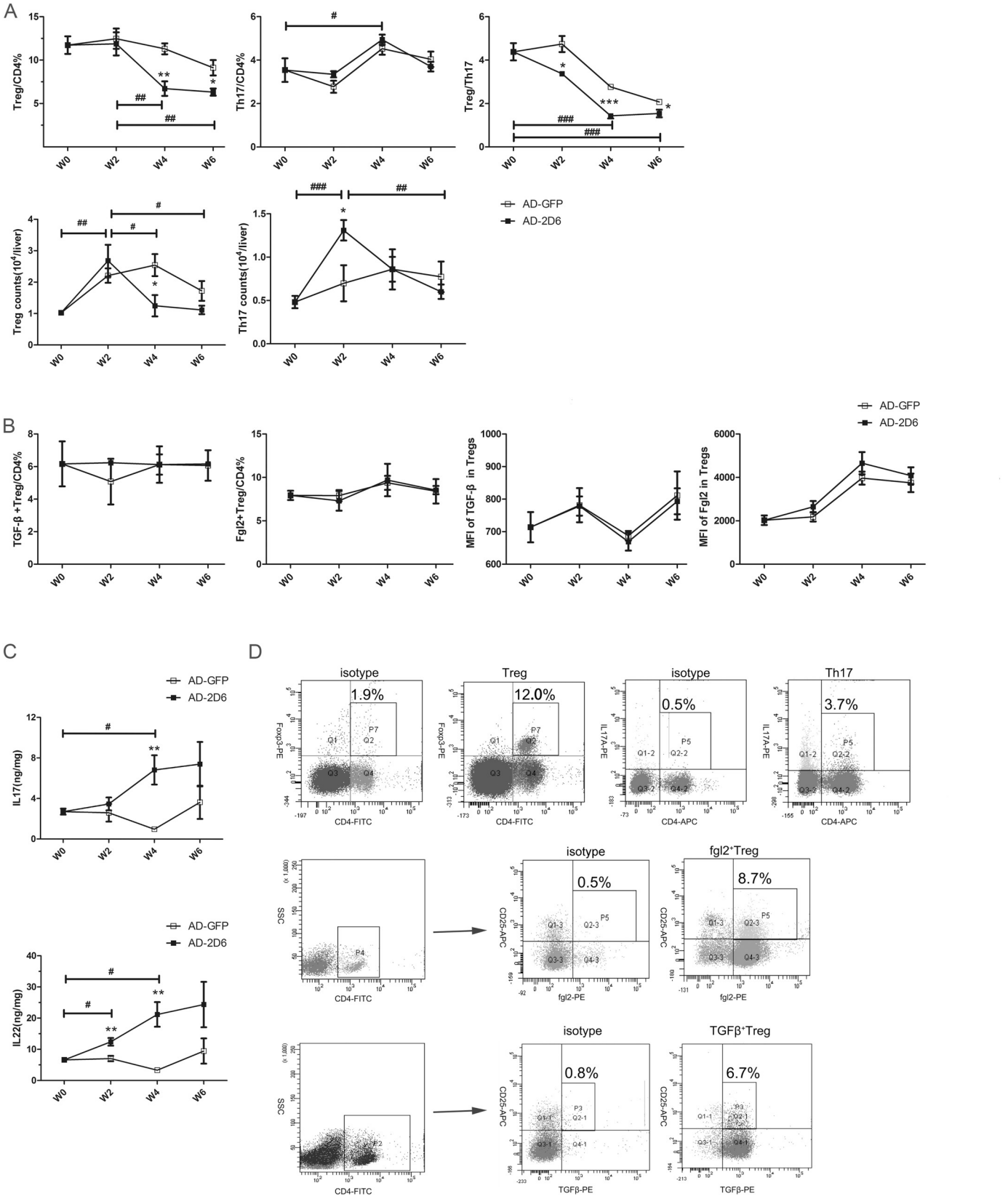

(caption on next page)

Fig. 2. Ratio of Treg/Th17 cells was significantly decreased in the liver of AD-2D6 mice. (A) The hepatic proportion of $CD4^+$ $FOXP3^+$ Tregs, $CD4^+$ $IL17A^+$ Th17 cells within $CD4^+$ T cells, the ratio of Treg/Th17 cells and the absolute numbers of hepatic $CD4^+$ $FOXP3^+$ Tregs, $CD4^+$ $IL17A^+$ Th17 cells in AD-2D6 mice and AD-GFP mice at 0 (before immunization), 2, 4 and 6 weeks after immunization. $^*p < 0.05$, $^{**}p < 0.01$, $^{***}p < 0.001$ compared between the two groups at the same time point. $^{\#}p < 0.05$, $^{\#\#}p < 0.01$, $^{\#\#\#}p < 0.001$ compared between different time points in the AD-2D6 group. (B) Comparison of the hepatic proportion of TGF-β^+ $CD4^+$ $CD25^+$ Tregs and $Fgl2^+$ $CD4^+$ $CD25^+$ Tregs within $CD4^+$ T cells, the mean fluorescent intensity (MFI) of TGF–β and Fgl2 in $CD4^+$ $CD25^+$ Tregs between AD-2D6 mice and AD-GFP mice. (C) The expression of hepatic IL 17 and IL 22 detected by ELISA of AD-2D6 mice and AD-GFP mice at 0 (before immunization), 2, 4 and 6 weeks after immunization. $^{**}p < 0.01$ compared between the two groups at the same time point. $^{\#}p < 0.05$, compared between different time points in the AD-2D6 group. (D) Representative flow cytometry staining of hepatic proportion of $CD4^+$ $FOXP3^+$ Tregs, $CD4^+$ $IL17A^+$ Th17 cells, TGF-β^+ $CD4^+$ $CD25^+$ Tregs, $Fgl2^+$ $CD4^+$ $CD25^+$ Tregs within $CD4^+$ T cells. $N = 5$/group/point-in-time.

were successfully infected with AD-2D6 (Fig. 1B). As mentioned in Meterial and Method 2.8, sections of rat livers and kidneys were used as substrates to detect serum LKM-1, an autoantibody specific to CYP2D6. Similar to patients with AIH-2, AD-2D6 mice generated LKM-1 autoantibody, which could be particularly evident by observed strong fluorescence staining in both rat livers and kidneys after incubation with sera from AD-2D6 mice, whereas serum samples from AD-GFP mice showed no reactivity at the dilutions tested (Fig. 1C). AD-2D6 mice showed a rapid increase in total IgG serum titers, which reached a peak at week 2 post infection. The levels of total IgG at weeks 2 and 4 were significantly higher in AD-2D6 mice than those observed in AD-GFP mice ($^*p = 0.0123$ and $^*p = 0.0252$, respectively) (Fig. 1D). The above-mentioned data indicate that AD-2D6 mice faithfully mirror human AIH and might be an appropriate AIH model for further investigation.

3.2. Ratio of Treg/Th17 cells was significantly decreased in the livers of AD-2D6 mice

To reveal the role of the hepatic Treg/Th17 balance in the development of AIH, we analyzed the proportions, absolute numbers, and related functional cytokine production in the liver. AD-2D6 mice showed a sustained decrease of Treg proportions (week 4 vs. week 2 and week 6 vs. week 2, $^{\#\#}p < 0.01$, $^{\#\#}p < 0.01$, respectively), an increased proportion of Th17 cells (week 4 vs. week 0, $^{\#}p < 0.05$), and a striking progressive decrease in the ratio of Treg/Th17 cells (week 4 vs. week 0 and week 6 vs. week 0, $^{\#\#\#}p < 0.001$, $^{\#\#\#}p < 0.001$, respectively). The proportion of Tregs among $CD4^+$ T cells (week 4 and week 6, $^{**}p < 0.01$, $^*p < 0.05$, respectively) and the ratio of Treg/Th17 cells (week 2, week 4, and week 6, $^*p < 0.05$, $^{***}p < 0.001$, $^*p < 0.05$, respectively) were significantly lower in AD-2D6 mice than those in AD-GFP mice, although their Th17 proportions were comparable during disease progression (Fig. 2A, D). In contrast to our expectation, AD-2D6 mice showed a transient increase in the number of Tregs (week 2 vs. week 0, $^{\#\#}p < 0.01$, respectively), but these cells rapidly decreased to a baseline level at week 6 (week 4 vs. week 2, week 6 vs. week 2, $^{\#}p < 0.05$, $^{\#}p < 0.05$). An obvious increase in Th17 cell count (week 2 vs. week 0, $^{\#\#\#}p < 0.001$), followed by a notable decline by week 6 (week 6 vs. week 2, $^{\#\#}p < 0.01$) was evident in AD-2D6 mice. Compared with AD-GFP mice, AD-2D6 mice had significantly lower Treg counts at week 4 ($^*p < 0.05$) and higher Th17 cell counts at week 2 ($^*p < 0.05$) (Fig. 2A). The transient increase in Tregs during the early stage of the disease in the AD-2D6 mice might reflect a compensatory mechanism to slow disease progression (Fig. 2A). Hepatic TGF-β-secreting or Fgl2-secreting Tregs were detected by flow cytometry, and effective cytokines of Th17 cells (IL-17 and IL-22) in hepatic homogenates were evaluated by ELISA. Although there were no obvious changes in the proportions or mean fluorescence intensity (MFI) of hepatic TGF–β and Fgl2 in $CD4^+$ $CD25^+$ Tregs (Fig. 2B), AD-2D6 mice had marked increases in concentrations of hepatic IL-17 (week 4 vs. week 0, $^{\#}p < 0.05$) and IL-22 (week 2 vs. week 0, and week 4 vs. week 0, $^{\#}p < 0.05$ and $^{\#}p < 0.05$, respectively). Moreover, compared with AD-GFP mice, AD-2D6 mice showed much higher hepatic IL-17 (week 4, $^{**}p < 0.01$) and IL-22 (week 2 and week 4, $^{**}p < 0.01$ and $^{**}p < 0.01$, respectively) levels (Fig. 2C). These data indicate that the balance of Treg/Th17 cells is disturbed in the AIH murine model.

3.3. Adoptive transfer of $CD4^+CD25^+$ T cells ameliorated liver injury in AD-2D6 mice

To confirm the critical contribution of the Treg/Th17 imbalance to the development of AIH in AD-2D6 mice, immunotherapy was administered to AD-2D6 mice by adoptive transfer of purified $CD4^+CD25^+$ T cells from healthy mice at weeks 2 and 3 post infection. The treated mice were sacrificed at week 4 (Fig. 3A–B). Compared with AD-2D6 mice treated with normal saline (N.S.), normal $CD4^+CD25^+$ T cells adoptively transferred into AD-2D6 mice effectively suppressed the infiltration of inflammatory cells into their livers, and resulted in ameliorated parenchyma hemorrhage and hepatocyte necrosis (Fig. 3C). Furthermore, we found that after this adoptive transfer therapy, the titers of serum total IgG ($^*p < 0.05$) and LKM-1 antibodies ($^*p < 0.05$) were much lower in $CD4^+CD25^+$ T cell-treated AD-2D6 mice than those in normal saline-treated AD-2D6 mice (Fig. 3D). As expected, a clear tendency toward an increase in Treg proportions and decrease in Th17 cell proportions, with significant higher Treg counts ($^*p < 0.05$), lower Th17 cell counts ($^*p < 0.05$), and obviously higher Treg/Th17 ratios ($^*p < 0.05$) were observed in the livers of $CD4^+CD25^+$ T cell recipients, compared with those of mice administered normal saline (Fig. 3E). Correspondingly, the $CD4^+CD25^+$ T cell-treated AD-2D6 mice showed a marked reduction in the expression of hepatic IL-17 ($^*p < 0.05$), and, although not significant, a trend of reduced hepatic IL-22 levels (Fig. 3F). These results indicate that immunotherapy with adoptively transferred $CD4^+CD25^+$ T cells could be in favor of correcting Treg/Th17 imbalance and preventing poor prognosis of AIH.

3.4. Proportions of Tregs in the periphery of AIH patients were various in different Child-Pugh classification

Sixteen AIH patients were included in the study to investigate whether an imbalance of peripheral Treg/Th17 cells contributed to the progression of human AIH. Demographic and biochemical characteristics of patients are shown in Table 1. All of the patients were serum positive for ANA antibody. Nine patients (56.25%) were graded Child-Pugh class A, and seven patients (43.75%) were allocated to class B or C [16]. The levels of alanine aminotransferase (ALT), aspartate aminotransferase (AST), alkaline phosphatase (ALP), and gamma-glutamyl transpeptidase (γ-GGT) were comparable between the two groups. Although no significant differences were found in the proportions of Th17 cells or the ratios of Treg/Th17 between AIH patients and healthy controls, peripheral Treg proportions were significantly different among AIH patients with different severities of liver damage, as determined by Child-Pugh classification. Compared with patients with Child-Pugh class A, patients with Child-Pugh class B or C showed significantly lower Treg proportions ($p = 0.041$) and a a trend of decreased Treg/Th17 ratios (Fig. 4A–B). Compared with normal liver tissue, liver biopsies from two AIH patients showed typical interface hepatitis and plasma cell infiltration (Fig. 4C). These results were consistent with those found in the AIH murine model and confirmed the role of Treg/Th17 balance in AIH.

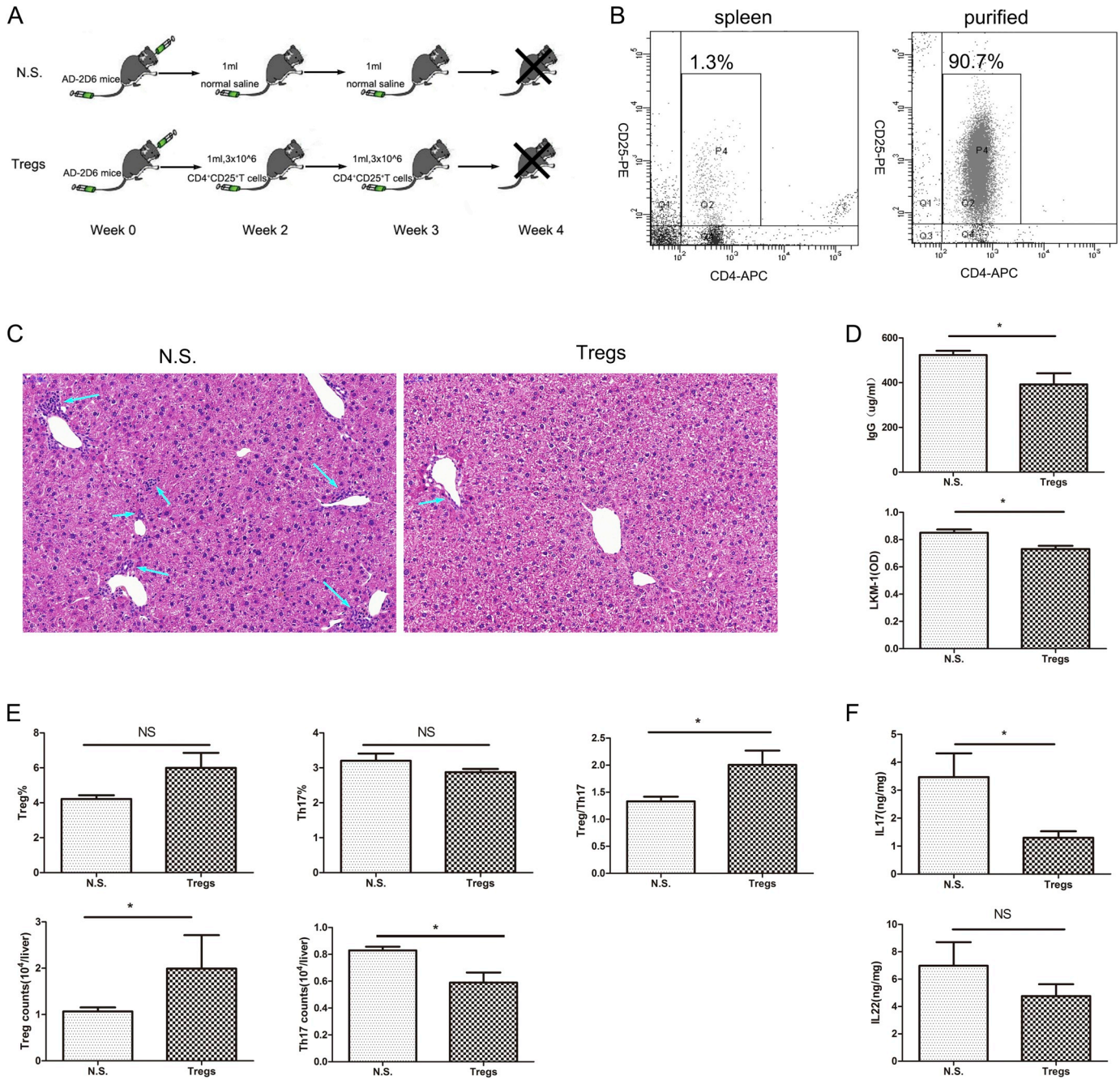

Fig. 3. Adoptive transfer of $CD4^+$ $CD25^+$ T cells ameliorated liver injury in AD-2D6 mice. (A) The schematic process of immunotherapy. (B) Flow cytometry staining showed the purity of $CD4^+$ $CD25^+$ Tregs isolated from splenocytes of healthy mice. (C) Representative HE staining of the liver tissue showed an obvious difference in interface hepatitis (green arrows) between AD-2D6 mice treated with $CD4^+$ $CD25^+$ Tregs and AD-2D6 mice treated with normal saline (N.S.) (magnification, × 200). (D) Comparison of the serum titers of total IgG and LKM-1 between the AD-2D6 mice treated with $CD4^+$ $CD25^+$ Tregs and AD-2D6 mice treated with N.S. $*p < 0.05$ compared between the two groups. (E) Comparison of the hepatic proportion of $CD4^+$ $FOXP3^+$ Tregs and $CD4^+$ $IL17A^+$ Th17 cells within $CD4^+$ T cells, the ratio of Treg/Th17 and the absolute numbers of hepatic $CD4^+$ $FOXP3^+$Tregs, $CD4^+$ $IL17A^+$ Th17 cells between the AD-2D6 mice treated with $CD4^+$ $CD25^+$ Tregs and AD-2D6 mice treated with N.S.. NS, nonsignificant differences between the two groups. $*p < 0.05$ compared between the two groups. (F) Comparison of the hepatic IL-17 and IL-22 expression between the AD-2D6 mice treated with $CD4^+$ $CD25^+$ Tregs and AD-2D6 mice treated with N.S.. NS, nonsignificant differences between the two groups. $*p < 0.05$ compared between the two groups. N = 5/group. (For interpretation of the references to colour in this figure legend, the reader is referred to the web version of this article.)

4. Discussion

Although AIH was originally described over 70 years ago [17], the immunopathogenesis of the disease remains unclear because there is no efficient and representative animal model. Researchers have made great efforts to develop an ideal animal model that mimics the development of AIH in humans. Compared with some early animal models of AIH, the novelty of the CYP2D6 model used in our study is that the adenovirus solution delivered into the livers of mice contains the human CYP2D6 gene, a defined major autoantigen in AIH-2 that can induce the production of high titers of specific anti-CYP2D6 antibodies (anti-LKM-1), which are thought to be the most important contributor to liver injury in AIH. Another advantage of the CYP2D6 model is that liver fibrosis progression can be observed with chronic hepatic

Table 1
The clinical characteristics of AIH patients and health controls.

Number	AIH patients		Health Controls	*p*-Values		
	Child-A (N = 9)	Child-B or C (*N* = 7)	HCs(N = 8)	A versus H	BC versus H	A versus BC
Age(years)	51.78 ± 2.948	47.57 ± 4.654	45.63 ± 0.375	NS	NS	NS
Gender (female%)	100%	100%	100%	–	–	–
ALT(U/L)	190.8 ± 109.0	97.43 ± 23.34	13.00 ± 1.102	NS	**	NS
AST(U/L)	174.0.3 ± 95.06	120.4 ± 34.69	18.88 ± 1.217	NS	**	NS
ALP(U/L)	261.7 ± 68.17	382.9 ± 90.94	47.38 ± 3.789	**	**	NS
γ-GGT(U/L)	435.8 ± 110.3	500.9 ± 202.7	14.38 ± 2.375	**	*	NS
ANA(%)	100%	100%	0%	–	–	–
LKM-1(%)	0%	0%	0%	–	–	–

Abbreviation: NS, nonsignificant.
* $p < 0.05$.
** $p < 0.01$ vs control group.

inflammation, although an increase in serum aminotransferase levels is absent [18]. In this study, we successfully established an AD-2D6 mouse model that displays representative features of AIH in humans, including interface hepatitis, elevated IgG serum titers, and the production of anti-LKM-1 autoantibodies. Most importantly, evidence from the animal model and AIH patients suggests that an imbalance of Treg/Th17 cells, characterized by decreased Treg proportion and Treg/Th17 ratio, as well as increased expression of IL-17 and IL-22, might contribute to inflammatory hepatic injury and could be corrected by adoptive transfer with healthy $CD4^+CD25^+$ T cells.

Recently, $CD4^+$ T lymphocytes that recognize autoantigenic epitopes presented by hepatocytes were identified as the drivers of autoimmune processes since they could trigger multiple specific immune responses [19,20]. Tregs and Th17 cells, two distinct $CD4^+$ T cell subsets derived from Th1 and Th2 cells, have opposite effects on autoimmune disease progression [9,21,22]. Progressive liver injury in AIH can be attributed to the breakdown of self-tolerance, and immune suppression mediated by professional Tregs is considered a key to control excessive inflammatory responses. However, the contribution of Tregs to this organ-specific autoimmune disease remains controversial [23]. There is a wealth of data that indicates Tregs are both numerically and functionally deficient in AIH patients versus healthy controls [24–26], supporting the idea that an immunoregulatory defect accounts for the unrestrained immune attack on the liver. In contrast, Tregs have been reported to be fully functional and not reduced in frequency in AIH [27]. In this study, we observed a numerically but not functionally deficient in hepatic Tregs.

Th17 cells are another T cell subset that exerts pro-inflammatory actions in AIH [28–30]. Evidence of this T cell subset as a critical player in AIH emerged from research showed that the level of IL-17 was much higher in an experimental autoimmune hepatitis (EAH) mice model than that in healthy controls [31]. Recent data have shown that in experimental models of AIH, mice deficient in either IL-17 [32] or the IL-17 receptor [33] are partially protected from hepatic injury, indicating that, as the major cellular source of IL-17, numerically or functionally changes of Th17 cells might greatly influence the disease progression. Increased IL-17 and IL-22 secretions were observed in the liver of AD-2D6 mice, futher supporting that AIH is a Th17-related autoimmune disease.

Tregs and Th17 cells appear to share common differentiation pathways.There is considerable developmental plasticity between the two cell subsets, even though they perform opposite functions, as Tregs can be reprogrammed to Th17 cells both in vitro and in vivo [34–36]. Recent studies have shown that Tregs can inhibit the proliferation of Th17 cells by secreting IL-35, and that Foxp3 could markedly diminish the transcription of retinoic acid-related orphan receptor-γt (ROR-γt) and retinoic acid-related orphan receptor-α (ROR-α), thereby limiting the differentiation of Th17 cells. In addition, all approaches to the inhibition of IL-17 might increase the expression of Foxp3 by Tregs, as well as their suppressive function [37]. Multiple studies have demonstrated relationships between the Treg/Th17 balance and autoimmune disease. In primary immune thrombocytopenia (ITP) patients, the peripheral ratio of Treg/Th17 cells was reduced and negatively correlated with disease activity [38,39]. The ratio of Th17-to-Treg cell frequency in peripheral circulation was increased in patients with pediatric psoriasis and positively correlated with disease severity [40]. Thus, the ratio of Treg/Th17 is regarded as a key factor in immune homeostasis and might be critical to autoimmune disease.

Emerging evidence suggests that the liver is an immunological organ with unique innate immune and immune tolerance properties. Given that the immunologic parameters in peripheral blood and bone marrow differ greatly from those in the liver [41], exploring regional immune features in the liver might be beneficial to understanding the immunopathogenesis of liver diseases. However, research on the relationship between hepatic regional immune features and the progression of AIH is limited at present. In this study, by establishing an AD-2D6-induced AIH mouse model, we followed the hepatic Treg/Th17 balance longitudinally, surveying relative numbers, absolute numbers, ratios, and representative functional molecules for both Tregs and Th17 cells. Akin to results from studies on other autoimmune diseases [38,42], we found that the hepatic Treg/Th17 balance skewed toward a Th17 response during AIH progression. Considering the dynamics of hepatic inflammatory changes, we speculated that the hepatic imbalance of Treg/Th17 cells might play a role in the pathogenesis of AIH. For AIH patients included in our study, the higher the Child-Pugh classification, the lower the Treg proportion and Treg/Th17 ratio, which partially confirmed the results obtained from mice. That we failed to detect a significant difference of Treg/Th17 ratios between AIH patients and volunteers might suggest a compensatory increase in Tregs allowed in the early stage of disease progression and a consequence of the failure to correct the decreased Treg/Th17 ratio due to poor hepatic reserve function in patients with higher Child-Pugh score. The above-mentioned explanation is also supported by the findings described in Result 3.2, in which AD-2D6 mice showed a transient increase in the number of Tregs at week 2, but rapidly decreased thereafter. Besides, the limited number of cases might result in a high degree of dispersion or variability in data and account for only change trend found between groups.

Treg-based therapies with freshly isolated or expanded Tregs could be an alternative solution to fight against autoimmune disease, much like standard immunosuppressive drugs they may replace [43]. Therapeutic effect of Tregs have been demonstrated in preclinical studies in various autoimmune disease models, including SLE [44], T1D [45], inflammatory bowel diseases [46], and autoimmune encephalomyelitis [47]. And > 280 clinical trials aimed at exploring the potential of Treg therapy, have been registered in clinicaltrials.gov [48]. Accordingly, infusion of Tregs also appears to be an effective means of restoring immunological tolerance to liver autoantigens and inhibiting cell-

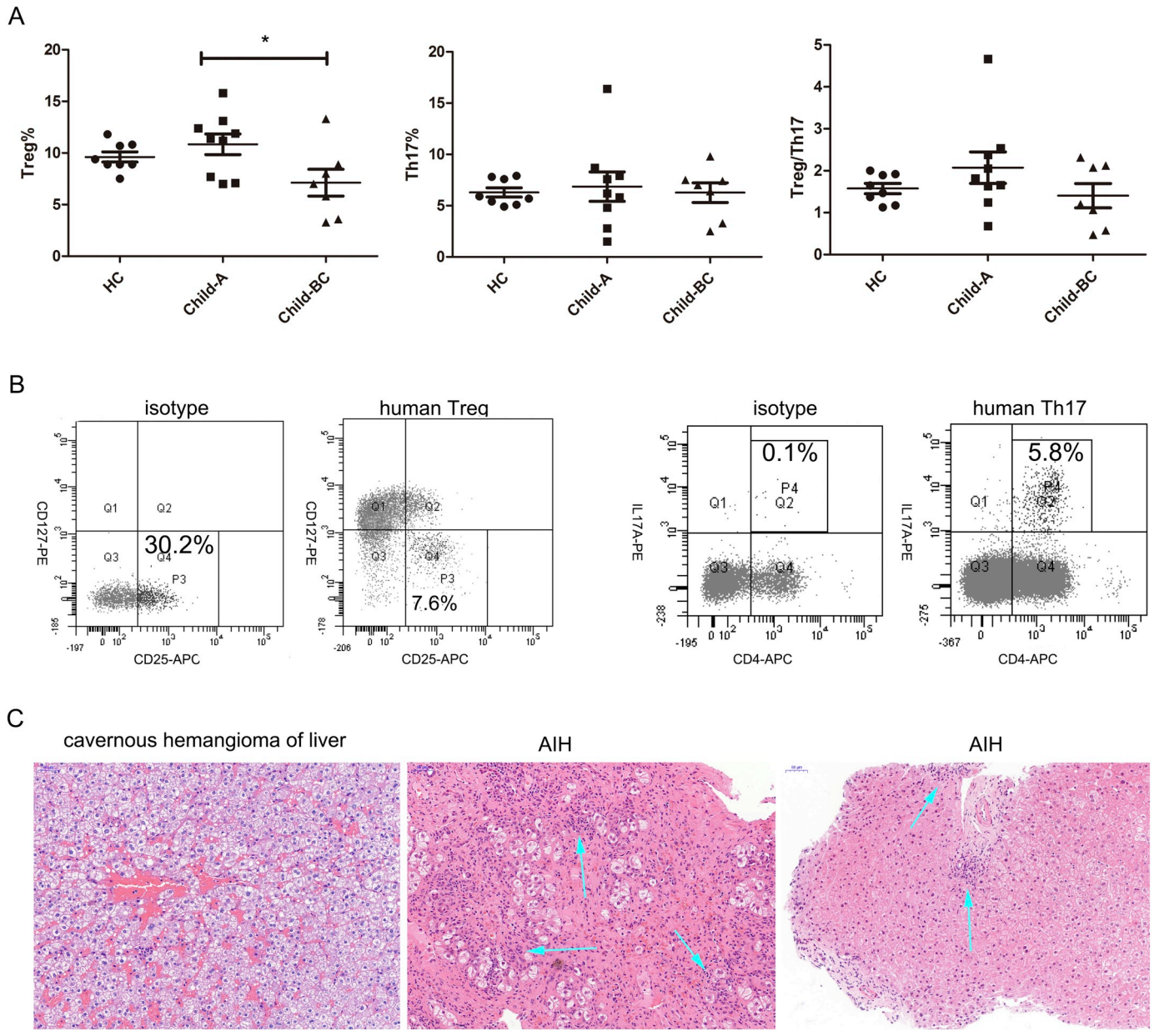

Fig. 4. Peripheral proportion of Tregs were various in AIH patients with different Child-Pugh classification. (A) Comparison of the peripheral proportion of $CD4^+$ $CD25^+$ $CD127^{low/-}$ Tregs, $CD4^+$ $IL17A^+$ Th17 cells within $CD4^+$ T cells and the ratio of Treg/Th17 cells among health controls ($N = 8$), AIH patients with Child-Pugh class A ($N = 9$), and AIH patients with Child-Pugh class B or C ($N = 7$). $^*p < 0.05$ compared between the two groups. (B) Representative flow cytometry staining of human peripheral $CD4^+$ $CD25^+$ $CD127^{low/-}$ Tregs, $CD4^+$ $IL17A^+$ Th17 cells within $CD4^+$ T cells. (C) HE staining of a normal liver tissue surrounding a hepatic cavernous hemangioma, and liver tissues from two AIH patients: a moderate interface hepatitis (blue arrows) was seen in both AIH patients (magnification, × 200). (For interpretation of the references to colour in this figure legend, the reader is referred to the web version of this article.)

mediated liver damage [49]. In the clinical trials to date, the optimal Tregs dose for therapy could be as high as 100–500 × 10^6 cells/kg [50]. In the current study, we treated the mice models with 3 × 10^6 cells considering their weight range from 20 to 25 g. Cell therapy with Tregs has some clear cellular and molecular pathways so far. Firstly, transferred Tregs recruited into the peripheral lymph nodes and expressed increased levels of adhesion molecules that may promote functional interactions with target cells [48]. Secondly, activated Tregs can accumulated and proliferate in the inflamed tissue post transfer to achieve long-lasting disease protection [51]. Lastly, adoptively transferred Tregs utilized multiple mechanisms to suppress immune responses. Adoptively transferred Tregs do not only suppressed adaptive T cell responses via a variety of cell contact dependent and independent mechanisms [52–55], but also inhibited the accumulation and activation of neutrophils, monocytes/macrophages, dendritic cells via their production of IL-10 and TGF-β [56]. Adoptive transfer of Tregs were also demonstrated to be capable of suppressing the cytotoxic activities, proliferation, cytokine production of NK and NKT cells by TGF-β or in a cell-to-cell contact manner [57,58]. Evidence supporting a potential role for Tregs in blunting humoral immune responses through suppressing B cell Ig production and class switch recombination [59]. All the rapidly accumulated evidence on Tregs involvement in immune regulation will help us understand the possible underlying mechanisms as to how an adoptive transfer of Tregs contributed to corrected balance of Treg/Th17, decreased LKM-1 autoantibody titer and slowed progression of AIH-related hepatic inflammatory changes in AD-2D6 mice.

There were some limitations to and caveats for our study. That remission of disease was not notable may be attributed to the

unsatisfactory purity Treg population obtained with the conventional isolation strategies, which is also one of principal hurdles remained for clinical use of Treg therapy. In addition, more patients should be involved in further study to validate the role of Treg/Th17 balance in AIH.

In conclusion, our findings suggest that numerically reduced Tregs and functionally enhanced Th17 cells contribute to the poor prognosis of AIH. Correcting the Treg/Th17 imbalance represents a potential therapeutic approach to AIH. Additional efforts should be made to elucidate the precise mechanisms underlying the Treg/Th17 imbalance that exists in AIH and to optimize Treg-based immunotherapies.

Funding

This work was supported by the National Natural Science Foundation of China (NSFC81571989), the "Thirteenth Five-Year Plan" National Major Science and Technology Special Project on Major Communicable Diseases (2017ZX10202201), and the ministry of education innovation team development plan (IRT14R20).

Conflicts of interest

None of the authors has any potential financial conflict of interest related to this manuscript.

References

[1] E.M. Hennes, et al., Simplified criteria for the diagnosis of autoimmune hepatitis, Hepatology 48 (2008) 169–176 (Baltimore, Md).
[2] R. Liberal, G. Mieli-Vergani, D. Vergani, Clinical significance of autoantibodies in autoimmune hepatitis, J. Autoimmun. 46 (2013) 17–24.
[3] M.P. Manns, E.F. Johnson, K.J. Griffin, E.M. Tan, K.F. Sullivan, Major antigen of liver kidney microsomal autoantibodies in idiopathic autoimmune hepatitis is cytochrome P450db1, J. Clin. Invest. 83 (1989) 1066–1072.
[4] D. Vergani, M.S. Longhi, D.P. Bogdanos, Y. Ma, G. Mieli-Vergani, Autoimmune hepatitis, Semin. Immunopathol. 31 (2009) 421–435.
[5] C.R. Grant, et al., Dysfunctional CD39(POS) regulatory T cells and aberrant control of T-helper type 17 cells in autoimmune hepatitis, Hepatology 59 (2014) 1007–1015 (Baltimore, Md).
[6] I. Shalev, et al., Targeted deletion of fgl2 leads to impaired regulatory T cell activity and development of autoimmune glomerulonephritis, J. Immunol. 180 (2008) 249–260 (Baltimore, Md: 1950).
[7] S. Sakaguchi, et al., Foxp3+ CD25+ CD4+ natural regulatory T cells in dominant self-tolerance and autoimmune disease, Immunol. Rev. 212 (2006) 8–27.
[8] J. Pene, et al., Chronically inflamed human tissues are infiltrated by highly differentiated Th17 lymphocytes, J. Immunol. 180 (2008) 7423–7430 (Baltimore, Md: 1950).
[9] R.P. Singh, et al., Th17 cells in inflammation and autoimmunity, Autoimmun. Rev. 13 (2014) 1174–1181.
[10] X. Peng, Y. Wang, L. Bai, The mechanism of Th17 cells in immunoinflammatory response of systemic lupus erythematosus, Immunol. J 28 (2012) 237–240,246.
[11] X. Xu, et al., Increased Th22 cells are independently associated with Th17 cells in type 1 diabetes, Endocrine 46 (2014) 90–98.
[12] R. Liberal, et al., CD39 mediated regulation of Th17-cell effector function is impaired in juvenile autoimmune liver disease, J. Autoimmun. 72 (2016) 102–112.
[13] M.S. Longhi, M.J. Hussain, W.W. Kwok, G. Mieli-Vergani, Y. Ma, D. Vergani, Autoantigen-specific regulatory T cells, a potential tool for immune-tolerance reconstitution in type-2 autoimmune hepatitis, Hepatology 53 (2011) 536–547 (Baltimore, Md).
[14] R. Liberal, et al., In autoimmune hepatitis type 1 or the autoimmune hepatitis-sclerosing cholangitis variant defective regulatory T-cell responsiveness to IL-2 results in low IL-10 production and impaired suppression, Hepatology 62 (2015) 863–875 (Baltimore, Md).
[15] E. Hintermann, J. Ehser, U. Christen, The CYP2D6 animal model: how to induce autoimmune hepatitis in mice, J. Vis. Exp 60 (2012) 1–7, https://doi.org/10.3791/3644.
[16] R.N. Pugh, I.M. Murray-Lyon, J.L. Dawson, M.C. Pietroni, R. Williams, Transection of the oesophagus for bleeding oesophageal varices, Br. J. Surg. 60 (1973) 646–649.
[17] J. Waldenstrom, The diagnostic importance of ACTH, Acta Endocrinol. 5 (1950) 235–242.
[18] U. Christen, E. Hintermann, Immunopathogenic mechanisms of autoimmune hepatitis: how much do we know from animal models? Int. J. Mol. Sci. 17 (2016).
[19] D. Vergani, G. Mieli-Vergani, Aetiopathogenesis of autoimmune hepatitis, World J. Gastroenterol. 14 (2008) 3306–3312.
[20] M. Hardtke-Wolenski, et al., Genetic predisposition and environmental danger signals initiate chronic autoimmune hepatitis driven by CD4+ T cells, Hepatology 58 (2013) 718–728 (Baltimore, Md).
[21] E.V. Lourenco, A. La Cava, Natural regulatory T cells in autoimmunity, Autoimmunity 44 (2011) 33–42.
[22] D. Zhang, E. Tu, S. Kasagi, P. Zanvit, Q. Chen, W. Chen, Manipulating regulatory T cells: a promising strategy to treat autoimmunity, Immunotherapy 7 (2015) 1201–1211.
[23] J.H. Buckner, Mechanisms of impaired regulation by CD4(+)CD25(+)FOXP3(+) regulatory T cells in human autoimmune diseases, Nat. Rev. Immunol. 10 (2010) 849–859.
[24] M.S. Longhi, Y. Ma, D.P. Bogdanos, P. Cheeseman, G. Mieli-Vergani, D. Vergani, Impairment of CD4(+)CD25(+) regulatory T-cells in autoimmune liver disease, J. Hepatol. 41 (2004) 31–37.
[25] M.S. Longhi, et al., Effect of CD4+ CD25+ regulatory T-cells on CD8 T-cell function in patients with autoimmune hepatitis, J. Autoimmun. 25 (2005) 63–71.
[26] M.S. Longhi, et al., Functional study of CD4+CD25+ regulatory T cells in health and autoimmune hepatitis, J. Immunol. 176 (2006) 4484–4491 (Baltimore, Md: 1950).
[27] M. Peiseler, et al., FOXP3+ regulatory T cells in autoimmune hepatitis are fully functional and not reduced in frequency, J. Hepatol. 57 (2012) 125–132.
[28] L. Zhao, et al., Interleukin-17 contributes to the pathogenesis of autoimmune hepatitis through inducing hepatic interleukin-6 expression, PLoS One 6 (2011) e18909.
[29] T. Korn, E. Bettelli, M. Oukka, V.K. Kuchroo, IL-17 and Th17 cells, Annu. Rev. Immunol. 27 (2009) 485–517.
[30] P. Bertolino, Interleukin-22, interleukin-17, and other cytokines: a wall is coming down, Hepatology 47 (2008) 345–348 (Baltimore, Md).
[31] H. Yu, et al., IL-17 contributes to autoimmune hepatitis, J. Huazhong Univ. Sci. Technolog. Med. Sci = Hua zhong ke ji da xue xue bao Yi xue Ying De wen ban = Huazhong keji daxue xuebao Yixue Yingdewen ban 30 (2010) 443–446.
[32] F. Lafdil, et al., Myeloid STAT3 inhibits T cell-mediated hepatitis by regulating T helper 1 cytokine and interleukin-17 production, Gastroenterology 137 (2009) 2125-2135.e2121-2122.
[33] T. Nagata, L. McKinley, J.J. Peschon, J.F. Alcorn, S.J. Aujla, J.K. Kolls, Requirement of IL-17RA in Con A induced hepatitis and negative regulation of IL-17 production in mouse T cells, J. Immunol. 181 (2008) 7473–7479 (Baltimore, Md: 1950).
[34] M. Ayyoub, et al., Human memory FOXP3+ Tregs secrete IL-17 ex vivo and constitutively express the T(H)17 lineage-specific transcription factor RORgamma t, Proc. Natl. Acad. Sci. U. S. A. 106 (2009) 8635–8640.
[35] K.S. Voo, et al., Identification of IL-17-producing FOXP3+ regulatory T cells in humans, Proc. Natl. Acad. Sci. U. S. A. 106 (2009) 4793–4798.
[36] A. Ueno, et al., Increased prevalence of circulating novel IL-17 secreting Foxp3 expressing CD4+ T cells and defective suppressive function of circulating Foxp3+ regulatory cells support plasticity between Th17 and regulatory T cells in inflammatory bowel disease patients, Inflamm. Bowel Dis. 19 (2013) 2522–2534.
[37] N. Komatsu, et al., Pathogenic conversion of Foxp3+ T cells into TH17 cells in autoimmune arthritis, Nat. Med. 20 (2014) 62–68.
[38] L. Ji, et al., The ratio of Treg/Th17 cells correlates with the disease activity of primary immune thrombocytopenia, PLoS One 7 (2012) e50909.
[39] M.S. Longhi, et al., Inhibition of interleukin-17 promotes differentiation of CD25(−) cells into stable T regulatory cells in patients with autoimmune hepatitis, Gastroenterology 142 (2012) 1526–1535 (e1526).
[40] L. Zhang, et al., Characterization of Th17 and FoxP3(+) Treg cells in paediatric psoriasis patients, Scand. J. Immunol. 83 (2016) 174–180.
[41] I.N. Crispe, The liver as a lymphoid organ, Annu. Rev. Immunol. 27 (2009) 147–163.
[42] X.S. Shao, et al., The prevalence of Th17 cells and FOXP3 regulate T cells (Treg) in children with primary nephrotic syndrome, Pediatr. Nephrol. 24 (2009) 1683–1690.
[43] W.J. Chae, A.L.M. Bothwell, Therapeutic potential of gene-modified regulatory T cells: from bench to bedside, Front. Immunol. 9 (2018) 303.
[44] K.J. Scalapino, Q. Tang, J.A. Bluestone, M.L. Bonyhadi, D.I. Daikh, Suppression of disease in New Zealand Black/New Zealand White lupus-prone mice by adoptive transfer of ex vivo expanded regulatory T cells, J. Immunol. 177 (2006) 1451–1459 (Baltimore, Md: 1950).
[45] R. Mukherjee, P. Chaturvedi, H.Y. Qin, B. Singh, CD4+CD25+ regulatory T cells generated in response to insulin B:9–23 peptide prevent adoptive transfer of diabetes by diabetogenic T cells, J. Autoimmun. 21 (2003) 221–237.
[46] C. Mottet, H.H. Uhlig, F. Powrie, Cutting edge: cure of colitis by CD4+CD25+ regulatory T cells, J. Immunol. 170 (2003) 3939–3943 (Baltimore, Md: 1950).
[47] A.P. Kohm, P.A. Carpentier, H.A. Anger, S.D. Miller, Cutting edge: CD4+CD25+ regulatory T cells suppress antigen-specific autoreactive immune responses and central nervous system inflammation during active experimental autoimmune encephalomyelitis, J. Immunol. 169 (2002) 4712–4716 (Baltimore, Md: 1950).
[48] C. Donnelly, et al., Optimizing human Treg immunotherapy by Treg subset selection and E-selectin ligand expression, Sci. Rep. 8 (2018) 420.
[49] H.X. Wei, et al., CD4+CD25+ Foxp3+ regulatory T cells protect against T cell-mediated fulminant hepatitis in a TGF-β-dependent manner in mice, J. Immunol. 181 (2008) 7221–7229.
[50] R. Duggleby, R.D. Danby, J.A. Madrigal, A. Saudemont, Clinical grade regulatory CD4(+) T cells (Tregs): moving toward cellular-based immunomodulatory therapies, Front. Immunol. 9 (2018) 252.
[51] H. Waldmann, R. Hilbrands, D. Howie, S. Cobbold, Harnessing FOXP3+ regulatory T cells for transplantation tolerance, J. Clin. Invest. 124 (2014) 1439–1445.
[52] A. Schmidt, N. Oberle, P.H. Krammer, Molecular mechanisms of treg-mediated T cell suppression, Front. Immunol. 3 (2012) 51.
[53] P.B. Ernst, J.C. Garrison, L.F. Thompson, Much ado about adenosine: adenosine synthesis and function in regulatory T cell biology, J. Immunol. 185 (2010)

1993–1998 (Baltimore, Md: 1950).
[54] W.J. Grossman, J.W. Verbsky, W. Barchet, M. Colonna, J.P. Atkinson, T.J. Ley, Human T regulatory cells can use the perforin pathway to cause autologous target cell death, Immunity 21 (2004) 589–601.
[55] M. Mizui, G.C. Tsokos, Targeting regulatory T cells to treat patients with systemic lupus erythematosus, Front. Immunol. 9 (2018) 786.
[56] K.J. Maloy, L. Salaun, R. Cahill, G. Dougan, N.J. Saunders, F. Powrie, CD4 + CD25 + T(R) cells suppress innate immune pathology through cytokine-dependent mechanisms, J. Exp. Med. 197 (2003) 111–119.
[57] F. Ghiringhelli, et al., CD4 + CD25 + regulatory T cells inhibit natural killer cell functions in a transforming growth factor-beta-dependent manner, J. Exp. Med. 202 (2005) 1075–1085.
[58] T. Azuma, T. Takahashi, A. Kunisato, T. Kitamura, H. Hirai, Human CD4 + CD25 + regulatory T cells suppress NKT cell functions, Cancer Res. 63 (2003) 4516–4520.
[59] H.W. Lim, P. Hillsamer, A.H. Banham, C.H. Kim, Cutting edge: direct suppression of B cells by CD4 + CD25 + regulatory T cells, J. Immunol. 175 (2005) 4180–4183 (Baltimore, Md: 1950).